

1  
2  
3  
4  
5  
6  
7  
8  
9  
10  
11  
12  
13  
14  
15  
16  
17  
18  
19  
20  
21  
22  
23  
24  
25

## Title

**Spatial analysis of COVID-19 spread in Iran: Insights into geographical and structural transmission determinants at a province level**

## Authors

\*Ricardo Ramírez-Aldana<sup>1</sup>, Juan Carlos Gomez-Verjan<sup>1</sup>, Omar Yaxmehen Bello-Chavolla<sup>1,2</sup>

## Institutions

<sup>1</sup>Research Division, Instituto Nacional de Geriatria, Mexico City, Mexico

<sup>2</sup>Department of Physiology, Facultad de Medicina, Universidad Nacional Autónoma de México, Mexico City, Mexico

**\*Corresponding Author:** Ramírez-Aldana R. **e-mail:** ricardoramirezaldana@gmail.com, Research Division, Instituto Nacional de Geriatria (INGER), Anillo Perif. 2767, San Jerónimo Lídice, La Magdalena Contreras, 10200, Mexico City, Mexico.

26

27

## ABSTRACT

28 The Islamic Republic of Iran reported its first COVID-19 cases by 19<sup>th</sup> February 2020,  
29 since then it has become one of the most affected countries, with more than 73,000 cases  
30 and 4,585 deaths to this date. Spatial modeling could be used to approach an  
31 understanding of structural and sociodemographic factors that have impacted COVID-19  
32 spread at a province-level in Iran. Therefore, in the present paper, we developed a spatial  
33 statistical approach to describe how COVID-19 cases are spatially distributed and to  
34 identify significant spatial clusters of cases and how socioeconomic and climatic features  
35 of Iranian provinces might predict the number of cases. The analyses are applied to  
36 cumulative cases of the disease from February 19<sup>th</sup> to March 18<sup>th</sup>. They correspond to  
37 obtaining maps associated with quartiles for rates of COVID-19 cases smoothed through a  
38 Bayesian technique and relative risks, the calculation of global (Moran's I) and local  
39 indicators of spatial autocorrelation (LISA), both univariate and bivariate, to derive  
40 significant clustering, and the fit of a multivariate spatial lag model considering a set of  
41 variables potentially affecting the presence of the disease. We identified a cluster of  
42 provinces with significantly higher rates of COVID-19 cases around Tehran (p-value<  
43 0.05), indicating that the COVID-19 spread within Iran was spatially correlated. Urbanized,  
44 highly connected provinces with older population structures and higher average  
45 temperatures were the most susceptible to present a higher number of COVID-19 cases  
46 (p-value < 0.05). Interestingly, literacy is a factor that is associated with a decrease in the  
47 number of cases (p-value < 0.05), which might be directly related to health literacy and  
48 compliance with public health measures. These features indicate that social distancing,  
49 protecting older adults, and vulnerable populations, as well as promoting health literacy,  
50 might be useful to reduce SARS-CoV-2 spread in Iran. One limitation of our analysis is that  
51 the most updated information we found concerning socioeconomic and climatic features is

52 not for 2020, or even for a same year, so that the obtained associations should be  
53 interpreted with caution. Our approach could be applied to model COVID-19 outbreaks in  
54 other countries with similar characteristics or in case of an upturn in COVID-19 within Iran.

55

56 **Keywords: COVID-19, Iran, SARS-CoV-2, spatial clusters, spatial epidemiology,**  
57 **spatial statistics.**

58

### 59 **Author Summary**

60 Iran was among the first countries reporting a rapid increase in the number of COVID-19  
61 cases. Spatial epidemiology is useful to study the spatial distribution of a disease and to  
62 identify factors associated with the number of cases of such disease. By applying these  
63 methods, we aimed to identify whether there are clusters of regions in Iran with high or low  
64 number of COVID-19 cases and the association of different factors with these numbers,  
65 considering spatial relationships and maps representing these associations. Interestingly,  
66 we found regions of high number of cases and that more COVID-19 cases were present in  
67 provinces with more urbanization, aging population, number of physicians, efficient  
68 communications, and greater average temperatures, whereas less COVID-19 cases were  
69 present in provinces with more literacy. This study allowed us to understand the spatial  
70 behavior of the disease and the importance of having adequate health policies, literacy  
71 campaigns, and disseminating health information to the population.

72

73

## 74 INTRODUCTION

75 On 11<sup>th</sup> March 2020, the General Director of the World Health Organization (WHO), Dr.  
76 Tedros Adhanom Ghebreyesus, declared the new infectious respiratory disease COVID-  
77 19, caused by the infection of novel coronavirus SARS-CoV-2 as a pandemic, due to the  
78 rate of growth of new cases, the number of affected people, and the number of deaths (1).  
79 As of the time of this writing (April 15<sup>th</sup>, 2020), the number of infected cases world-wide  
80 corresponded to more than 1 million, being the most affected countries: Italy (16,523  
81 deaths), Spain (13,341 deaths), USA (10,792 deaths), France (8,911 deaths), United  
82 Kingdom (5,373 deaths), and Iran (3,739 deaths)(2,3).

83 Iran was among the first countries outside of China to report a rapid increase in the  
84 number of COVID-19 cases and associated deaths; its first confirmed cases were reported  
85 on 19th February 2020 in the province of Qom imported from Wuhan, China(4).  
86 Nevertheless, some reports suggest that the outbreak may have happened two or six  
87 weeks before the government official announcement (5). Iran had one of the highest  
88 COVID-19 mortality rates early in the pandemic, and its rate of spread has been amongst  
89 the highest. However, as with other countries, it may be a sub-estimation of cases, and  
90 there may be other cases not officially reported (6).

91 The large count of COVID-19 cases and mortality in Iran are multifactorial. Iran's response  
92 to the epidemic has been highly affected by several imposed economic sanctions and  
93 armed conflicts within the last 20 years. Moreover, its difficult economic situation due to a  
94 recession, having inflation rates that are among the highest in the region, has taken a toll  
95 on its public health system (7,8). Although there are approximately 184,000 hospitals and  
96 primary health-care staff, limitations in the availability of COVID-19 testing kits, protective  
97 equipment, and ventilators are quite important. On the other hand, over the last years, Iran  
98 has slowed the rate of mortality associated with infectious and maternal diseases. It is  
99 currently undergoing an epidemiological transition where infectious diseases interact with

100 chronic conditions (2). In this sense, Iran may represent other similar developing world  
101 countries with poor health systems and an increased prevalence of chronic diseases.  
102 Spatial statistics have emerged as a useful tool for the analysis of spatial epidemiology,  
103 concerning mapping and statistical analyses of spatial and spatial-temporal incidences of  
104 different pathogens. The aim of this paper is to perform spatial analyses which allow us to  
105 better understand the COVID-19 outbreak in Iran, not only in terms of the strength of its  
106 presence and socioeconomic and structural factors which facilitate the disease spread  
107 within Iranian provinces, but also in terms of how the disease is spatially distributed and  
108 which variables are spatially related with it considering the spatial effect to obtain adequate  
109 inferences. Given the role of climate and socio-economic factors in determining the  
110 distribution of cases and its impact world-wide, we also aimed to incorporate said factors  
111 as predictors of SARS-CoV-2 spread (9,10). This could aid to understand the burden of  
112 COVID-19, its distribution in the country, and its implication on public health within Iran and  
113 similar countries (11) and could contribute to public health measures by providing insight  
114 to inform the implementation of interventions or to understand socio-demographic factors  
115 associated with the SARS-CoV-2 spread and COVID-19 heterogeneity as it has been  
116 applied to previous infectious diseases (12–16).

## 117 **MATERIAL AND METHODS**

### 118 Data sources

119 We obtained province-specific data considering 31 provinces or polygons in Iran (**Table 1**).  
120 From the Statistical Centre of Iran (17), we extracted information concerning: 1) people  
121 settled in urban areas in 2016 (%), calculated from the population and household of Iran  
122 by province and sub-province information of the census, 2) people aged  $\geq 60$  years in 2016  
123 calculated from the population disaggregated by age groups, sex, and province  
124 information of the census, 3) population density (people per  $km^2$ ) in 2016, 4) literacy rate  
125 of population aged  $\geq 6$  years in 2016, obtained from the document of selected results from

126 the 2016 census, 5) the Consumer Price Index percent changes on March 2020 for the  
127 national households in contrast to the corresponding month of the previous year (point-to-  
128 point inflation), and 6) the average temperature (°C) of provincial capitals and 7) annual  
129 precipitation levels (mm) in 2015, both part of the climate and environment information.  
130 From the Iran data portal (18), we obtained, from the health section: 1) the number of  
131 physicians employed by the ministry of health and medical education in 2006 and 2) the  
132 number of beds in operating medical establishments in 2006 and from the government  
133 finance section: 3) the province contribution to gross domestic product (GDP) in 2004. We  
134 used a Transportation Efficiency Index (TEI)(19), constructed through Data Evelopment  
135 Analysis, being an indicator of the extent in which each province efficiently utilize their  
136 transportation infrastructure. The TEI has values between zero and one, values near to  
137 one indicate provinces better communicated, but we standardized it (values of each  
138 province minus its mean divided by the associated standard deviation) to allow  
139 interpretations in a better scale in terms of how the increase in a certain number of  
140 standard deviations of the TEI is associated with the number of COVID-19 cases. The  
141 cumulative number of cases with confirmed COVID-19 by Province from February 19<sup>th</sup> to  
142 March 18<sup>th</sup>, 2020, was also obtained (20). It is important to notice that, in order to obtain  
143 more accurate rates of cases with COVID-19, population size in 2020 by province was  
144 derived by using mathematical projection methods (arithmetic, geometric, exponential, and  
145 logistic or saturation methods) using information contained in the population and housing  
146 censuses from 2006, 2011, and 2016. Since all methods provided similar results, we show  
147 here only those associated with the arithmetic method. Shapefiles were obtained from the  
148 Stanford Libraries Earthworks: [https://earthworks.stanford.edu/catalog/stanford-](https://earthworks.stanford.edu/catalog/stanford-dv126wm3595)  
149 [dv126wm3595](https://earthworks.stanford.edu/catalog/stanford-dv126wm3595), in which files are freely available for academic use and other non-  
150 commercial use (21).

151 *COVID-19 rate estimation by Iranian provinces*

152 We obtained quantile maps associated with raw rates of COVID-19 cases, as well as  
153 smoothed case rates by province using an empirical Bayes estimator, which is a biased  
154 estimator that improves variance instability proper of rates estimated in small-sized spatial  
155 units (22) (i.e. provinces with a larger population size have lower variance than provinces  
156 with a smaller population size). Since raw and smoothed rates were surprisingly similar,  
157 only results of smoothed rates are reported. We also obtained maps concerning excess or  
158 relative risk, serving as a comparison of the observed number of cases by the province to  
159 a national standard. For the variable concerning the number of people aged  $\geq 60$  years by  
160 province, raw, and smoothed rates were obtained using empirical Bayes, and the latter  
161 were used in all analyses.

#### 162 *Spatial weight estimation and spatial autocorrelation*

163 Since all spatial analyses require spatial weights, we obtained queen contiguity weights  
164 (23). Provinces were considered as neighbors when they share at least a point or vertex in  
165 common, obtaining a squared matrix of dimension 31 (31x31 matrix) with all entries equal  
166 to zero or one, the latter value indicating that two provinces are neighbors. From these  
167 neighbors, weights are calculated by integrating a matrix in a row-standardized form, i.e.,  
168 equal weights for each neighbor and summing one for each row. Moran's I statistic was  
169 obtained as an indicator of global spatial autocorrelation (24), and its significance was  
170 assessed through a random permutation inference technique based on randomly  
171 permuting the observed values over the spatial units (25). Local indicators of spatial  
172 autocorrelation (LISA) were obtained, being these a decomposition of Moran's I used to  
173 identify the contribution of each province in the statistic (26). LISA was used to derive  
174 significant spatial clustering through four cluster types: High-High, Low-Low, High-Low,  
175 and Low-High. For instance, the High-High cluster indicates provinces with high values of  
176 a variable that are significantly surrounded by regions with similarly high values.  
177 Analogous to Moran's I and LISA, estimates can be calculated to identify the spatial

178 correlation between two variables and to identify bivariate clustering (27). For instance, to  
179 identify provinces with high values in a first variable surrounded by provinces with high  
180 values for a second variable (cluster High-High). Bivariate clustering and quartile maps  
181 were obtained for each of the significant variables in a linear spatial model, to have a  
182 better understanding of the individual spatial effect of each of these variables over the  
183 smoothed rates associated with the disease.

#### 184 *Spatial multivariate linear models*

185 Spatial multivariate linear models were fitted to identify variables that significantly impact  
186 the  
187 number of log-transformed COVID-19 cases (28). This response variable was chosen  
188 since  
189 the corresponding model better satisfies all statistical assumptions, the other variables  
190 introduced in the Data section were simultaneously introduced as explanatory, first  
191 removing from the model all variables generating multicollinearity. Ordinary Least Squares  
192 (OLS) estimation was used to identify whether a linear spatial model was necessary by  
193 using a Lagrange Multiplier (LM) and a robust LM statistics to compare the non-spatial  
194 model with spatial models (29). Two kinds of spatial models were compared; the spatial-  
195 lag model considers the spatially lagged response as an additional explanatory variable,  
196 whereas the spatial-error model considers that the error is a linear function of a spatially  
197 lagged error plus another error term. Another model was obtained by performing a  
198 backward selection process, considering the elimination of the most non-significant  
199 variable in each step and the minimization of the Akaike Information Criterion (AIC). This  
200 process allowed us to identify whether the associations obtained through this model were  
201 similar as those obtained through the model including all variables. For significant  
202 variables in the linear spatial models, interpretations in the original scale (i.e., as counts)  
203 were derived and we performed bivariate LISA significant clustering between each of



204 these significant variables and the rate of cases with COVID-19, as explained above. All  
205 statistical analyses were conducted using GeoDa version 1.14.0. A two-tailed p-  
206 value<0.05 was considered as the significance threshold.

## 207 **RESULTS**

### 208 *Rates description and spatial autocorrelation of COVID-19 case rates between provinces*

209 Maps for quartiles corresponding to the smoothed rates and excess risk of COVID-19  
210 cases are shown in **Figure 1**. We observed that the highest rates of COVID-19 and excess  
211 risk values were located in the Northern region of Iran corresponding to the provinces of  
212 Qom, Marzaki, Mazandaran, and Semnan. There were also high rates associated with the  
213 provinces of Alborz, Gilan, Qazvin, and Yazd (last quartile). We observed significant  
214 spatial autocorrelation (Moran's  $I=0.426$ ,  $p=0.002$ ), indicating that COVID-19 rates  
215 between provinces are significantly spatially related. From the heat and significance maps  
216 corresponding to significant clusters using an empirical Bayes spatial technique, we  
217 delimited a High-High cluster in red, indicating a northern zone around Tehran and Alborz  
218 with significant high COVID-19 rates surrounded by areas with similarly high rates.  
219 Conversely, we delimited a Low-Low cluster in blue indicating southern provinces with  
220 small rates surrounded by areas with similarly lower rates, which includes the provinces of  
221 Bushehr, Homozgan, Sistan, and Baluschestan. Interestingly, Golestan showed in light  
222 purple, has significantly lower COVID-19 rates despite being surrounded by a cluster of  
223 provinces with higher rates (**Figure 2**).

### 224 *Selection of multivariate linear spatial model for COVID-19 spread*

225 Since the variable hospital beds is strongly associated with variables GDP and number of  
226 physicians (Kendall correlation coefficients above 0.55), we eliminated it from all models to  
227 avoid multicollinearity (Supplementary material). We confirmed that a spatial model was  
228 necessary since the error term from the OLS fitting showed significant spatial  
229 autocorrelation (Moran's  $I= 0.134$ ,  $p\text{-value}=0.025$ ). Additionally, the LM and Robust LM

230 statistics indicated that a spatial lag model was required since the spatial parameter ( $\rho$ )  
231 associated with the spatially lagged response was significant (LM=10.669, p-value=0.001;  
232 Robust LM=13.557, p-value < 0.001), which did not occur with the spatial error model  
233 since the corresponding spatial parameter was not consistently significant (LM=1.256, p-  
234 value=0.262; Robust LM=4.144, p-value=0.042). Thus, only the spatial lag model was  
235 fitted obtaining a significant spatial parameter ( $\rho = 0.723$ , p-value<0.001), which indicated  
236 that the rate of an area in the linear model is affected by COVID-19 rates in neighboring  
237 areas ( $R^2=0.877$ ,  $\sigma^2=0.146$ ). Normality and homoscedasticity assumptions were  
238 reasonably satisfied.

### 239 *Predictors of COVID-19 spatial spread in Iranian provinces*

240 The significant variables associated with the model obtained through the selection scheme  
241 were the same as those associated with the model including all variables. This simplified  
242 model excluded population density, Consumer Price Index, and annual precipitation. The  
243 estimated coefficients were similar for both models; however, we analyzed the estimations  
244 associated with the model including all variables to consider effects controlled for these  
245 three variables. Hence, the variables that significantly impact the log-transformed number  
246 of COVID-19 cases include: the percentage of people settled in urban areas (p-value =  
247 0.019), smoothed rate of people aged  $\geq 60$  years (p-value < 0.001), literacy rate (p-value =  
248 0.006), average temperature (p-value < 0.001), number of physicians employed (p-value <  
249 0.001), and the TEI (p-value = 0.035) (**Table 2**). A 10% increase in urban population or a  
250 1% increase in the population aged  $\geq 60$  years has a percentage increase of 29.29%  
251 (95%CI 26.55 – 32.10%) and 46.65% (95%CI 26.54% -69.95%), respectively, on the  
252 number of COVID-19 cases. Moreover, an increase of 1°C in the temperature levels, an  
253 increase of 1 physician, or an increase of one deviation over the standardized TEI also  
254 have a percentage increase of 11.98% (95%CI 5.54-18.80%), 0.08% (95%CI 0.06 -  
255 0.11%), and 16.98% (95%CI 1.14-35.30%), respectively, over the number of COVID-19

256 cases. Finally, a 1% increase in the literacy rate showed a percentage decrease of 10.44%  
257 (95%CI 3.18-17.16%) on the number of cases.

### 258 *Spatial lag predictors and province clusters*

259 Quartile maps for each of the significant variables in the spatial lag model are shown in  
260 **Figure 3**. Finally, concerning bivariate LISA significant clustering, we observed a positive  
261 spatial relationship (Moran's  $I=0.341$ ,  $p\text{-value}=0.002$ ) between urban population and  
262 COVID-19 rates; provinces with high urban rates surrounded by areas with high COVID-19  
263 rates are the same as the ones in the High-High cluster for COVID-19, except for  
264 Mazandaran, and similarly for the Low-Low cluster, except for Bushehr. There is also a  
265 positive spatial relationship (Moran's  $I=0.279$ ,  $p\text{-value}=0.002$ ) between the population aged  
266  $\geq 60$  and COVID-19 rates. Both High-High and Low-Low clusters include similar provinces  
267 as the ones in the clusters for COVID-19, except for Qom and Alborz, which have  
268 significantly lower rates of people aged  $\geq 60$  years but are spatially surrounded by areas  
269 with high disease rates. Concerning literacy rates, we also identified a positive spatial  
270 relationship between literacy and disease rates (Moran's  $I=0.362$ ,  $p\text{-value}=0.005$ ). The  
271 associated High-High cluster and that obtained for COVID-19 rates are formed by the  
272 same provinces, whereas in the south, Hormozgan and Bushehr have high literacy rates  
273 but are surrounded by areas with low disease rates.

274 Concerning average temperature levels, the global spatial autocorrelation is negative  
275 (Moran's  $I=-0.107$ ,  $p\text{-value}=0.103$ ). The High-High clusters for temperature and COVID-19  
276 rates are similar, except for Marzaki and Alborz, where there is significantly lower  
277 temperature surrounded by areas with high COVID-19 rates. In the south, there is a  
278 significantly high temperature with spatially lower disease rates.

279 There is a positive spatial relationship (Moran's  $I=0.302$ ,  $p\text{-value}=0.003$ ) between the  
280 number of physicians and the COVID-19 rate. There is a High-High cluster in the north  
281 with a High-Low zone between formed by Marzaki, Qom, and Semnan, with a significantly

282 lower number of physicians; however, they are spatially surrounded by areas with higher  
283 disease rates. Concerning the TEI, the spatial correlation is close to zero (Moran's  $I = -$   
284  $0.096$ ,  $p\text{-value}=0.112$ ), indicating a particular random global spatial relationship between  
285 TEI and the disease rate. The High-High cluster is the same as the High-High cluster for  
286 the disease, except for Mazandaran and Alborz, which have significantly low TEI but are  
287 surrounded by areas with high disease rates. In the south, two provinces, which formed a  
288 Low-Low cluster for COVID-19 cases, are now areas with high TEI spatially associated  
289 with areas with low disease rates.

## 290 **DISCUSSION**

291 Here, we demonstrate that the rates of COVID-19 cases within Iranian provinces are  
292 spatially correlated. This could be due to the origin of the outbreak, which started on the  
293 north of Iran, and can be seen through an important province cluster with the highest  
294 number of COVID-19 cases that we found around Tehran and Qom. Several  
295 mathematical models have been used to model the COVID-19 outbreak, mostly focused  
296 on forecasting the number of cases and assessing the capacity of country-level healthcare  
297 systems to manage disease burden (30–32). In the present report, we demonstrate that  
298 the spatial relationship and socio-demographic factors associated with the provinces must  
299 be considered to model the disease adequately, and this report also highlights structural  
300 factors that may lead to inequities in COVID-19 spread. Of relevance, we highlight the role  
301 of social determinants of health in sustaining SARS-CoV-2 transmission and provide  
302 additional evidence that human mobility or province interconnectedness might be  
303 associated in favoring disease spread (33).

304 Importantly, our approach demonstrates that urbanization, aging population, education,  
305 average temperatures, number of physicians, and inter-province communications are  
306 associated with the case numbers amongst Iranian provinces. The obtained results do not  
307 consider the spatial effect, which is accumulated since the spatially lagged response is

308 part of the explanatory variables, and they consider fixed values for all variables except the  
309 one being interpreted. Overall, these variables spatially correlate with the COVID-19  
310 province clustering indicating a consistent association with the observed variables. The  
311 greatest increase in the number of COVID-19 cases is associated with people aged  $\geq 60$   
312 years, urban population, and how well the provinces are communicated, with age having  
313 one of the most important associations, an increase of 1% in the corresponding rate  
314 implies a percentage increase of 46.65% over the number of cases. Of relevance,  
315 mortality attributable to COVID-19 complications is higher in this age group, and age  
316 increases the likelihood of developing the symptomatic disease and increased disease  
317 severity (34,35). Nevertheless, the association with older age could have different  
318 meanings depending on the number of comorbidities, with some reports labeling COVID-  
319 19 as an age-related disease (36). Our data demonstrate that the spatial spread of  
320 COVID-19 has a relationship with population aging structures, a concept that must be  
321 explored in this setting to obtain population-specific estimates and lethality and which  
322 could represent a significant structural inequality related to COVID-19 burden (37).

323 Urbanization rates also are associated with a percentage increase over the number of  
324 COVID-19 cases; we observed a similar association regarding province  
325 interconnectedness, which goes in line with recent information on human mobility and its  
326 effect in decreasing disease spread through social distancing (33). Urbanization, as a  
327 demographic phenomenon, leads to increased interconnectedness and human mobility as  
328 well as increased population density; these two factors facilitate disease spread. Emerging  
329 zoonotic diseases similar to SARS-CoV-2 have been linked to major structural factors that  
330 have been reported in other studies, including population growth, climate change,  
331 urbanization, and pollution (38,39). Thus, communication and the degree of urbanity, and  
332 what this implies in terms of pollution, overcrowding, among other factors, seem to be  
333 relevant to determine the number of COVID-19 cases and should imply geographical

334 targets for public health interventions to monitor disease spread and disease containment  
335 (40).

336 The only effect associated with a decrease in the number of COVID19 cases in our study  
337 was attributed to literacy, which might reflect several factors that ultimately influence  
338 disease spread. Data from several countries, including Iran, identified that higher health  
339 literacy was associated with a lower number of COVID-19 cases, probably reflecting  
340 attitudes towards public health measures including social distancing, early disease  
341 detection, and hand hygiene (41,42). Interestingly, this poses a potential public health  
342 intervention given that individuals with reduced health literacy, not only might have higher  
343 rates of COVID-19, but also increased likelihood for depression and impaired quality of life  
344 in suspected cases. Literacy's protective effect on disease spread also indicates a strong  
345 influence on social inequity and vulnerability as risk factors for COVID-19 spread,  
346 particularly on the influence of health equity, which will likely define the long-term impact of  
347 COVID-19 in many developing countries (43).

348 Concerning average temperature levels, we were able to obtain information associated  
349 only with the capitals and not the provinces, being a limitation of the analyzed information,  
350 obtaining some inconclusive results. On one hand, the global spatial autocorrelation was  
351 negative, though not statistically significant, indicating that global areas with higher  
352 temperatures are spatially related to areas with lower disease rates. On the other hand, on  
353 the spatial linear model, we derived that more temperature is associated with more cases.  
354 However; the former result does not contradict the latter since the direct effect in each  
355 province of a variable over the response is different from the spatial relationship between  
356 two variables. The latter considers one of the variables as spatially lagged (COVID-19),  
357 and thus the direct effect between variables in the same province is not included. In fact,  
358 this problem occurs in all the bivariate analysis, so care should be taken in all the  
359 interpretations. Notably, our results are consistent with previous analyses which have

360 analyzed the impact of climate on SARS-CoV-2 stability and spread (44). However, these  
361 results should be further studied considering the climate data limitations, that we obtained  
362 mixed results, and that some studies suggest there is no evidence that spread rates of the  
363 disease decline with higher temperatures (45).

364 Our study had some strengths and limitations. We approached COVID-19 using spatial  
365 analysis, which allowed us to identify province-level factors that are associated with the  
366 disease spread and which may be shared by other countries with similar socioeconomic or  
367 geographic structures by potentially identifying targets for country-wide public health  
368 interventions. This approach considers disease spread beyond individual-specific factors  
369 and could also be used to monitor areas of a potentially high number of undiagnosed  
370 cases that could facilitate disease spread and the surge of delayed waves of COVID-19  
371 after initial mitigation (46,47). Methodologically, all our analyses consider the spatial nature  
372 of the data. We identified significant spatial clustering and in terms of the spatial  
373 multivariate linear model, by including a spatial effect, we consider that the number of  
374 cases in an area is affected by those in neighboring areas. In this way, a lack of  
375 independency between spatial units is considered, being independence assumed in a  
376 usual linear model, thus obtaining more precise estimations. Of course, other statistical  
377 methods are available for this task, as generalized linear mixed models or geographically  
378 weighted regression; however, they do not use spatial weights, making our results more  
379 comparable with the Moran's I or spatial clustering, which are based on such weights. A  
380 limitation of our approach is that most of the variables used to explain COVID-19 disease  
381 rates were taken from previous years and not updates, given the unavailability of recent  
382 estimates. Furthermore, smoothed COVID-19 rates were calculated using a projection of  
383 the population in 2020 since the most recent census corresponds to 2016, thus rates could  
384 have slightly different values. In this sense, the explanatory variables were not projected  
385 since information of previous years was not always available; however, precise projections

386 for each variable were out of the scope of this work; and, it is also possible that some  
387 variables have a time lagged effect over the response. However; the time lagged effect we  
388 included was unintentional and dependent on the information available and not  
389 considering a lagged time effect as defined by experts; for instance, for GDP we used a  
390 time lag of 16 years, when perhaps it should have been of fewer years. When obtaining  
391 estimates using both projected and population size in 2016, we observed no significant  
392 changes in the results, which confirms the robustness of our approach. In fact, with all the  
393 mathematical projection methods similar results were obtained. However, the projections  
394 by province could be improved by considering a demographic balance equation and  
395 probabilistic projection methods as the ones obtained by country by the UN (48). In this  
396 sense, we suspect similar results would still be obtained since our projected values by  
397 country are similar to those obtained by the UN. We also observed that the smoothed and  
398 raw rates of COVID-19 cases were similar, with an absolute difference between them of at  
399 most 0.607 (considering rates for every 1000 individuals), this was probably due to Iran not  
400 having provinces with extremely small or large population size. Future work could be  
401 focused on evaluating spatio-temporal modeling, which could be useful to monitor disease  
402 spread and identify additional factors relating not only to transmission rates but also to  
403 transmission dynamics. Since COVID-19 is currently challenging health systems all over  
404 the world, science-centered public health decisions could benefit from spatial modeling to  
405 investigate larger factors targeted for public health interventions.

406 In conclusion, COVID-19 spread within Iranian provinces is spatially correlated. The main  
407 factors associated with a high number of cases are older age, high degrees of  
408 urbanization, province interconnectedness, higher average temperatures, lower literacy  
409 rates, and the number of physicians. Structural determinants for the spread of emerging  
410 zoonotic diseases, including SARS-CoV-2, must be understood in order to implement



411 evidence-based regional public health policies aimed at improving mitigation policies and  
412 diminishing the likelihood of disease re-emergence.

#### 413 **ORCID**

414 Ricardo Ramírez-Aldana: 0000-0003-4344-2928

415 Juan Carlos Gómez-Verján: 0000-0001-7186-8067

416 Omar Yaxmehen Bello-Chavolla: 0000-0003-3093-937X

417

#### 418 **Conflict of Interest:**

419 Nothing to disclose.

#### 420 **Funding:**

421 This project was supported by a grant from the Secretaría de Educación, Ciencia,  
422 Tecnología e Innovación de la Ciudad de México CM-SECTEI/041/2020 “Red  
423 Colaborativa de Investigación Traslacional para el Envejecimiento Saludable de la Ciudad  
424 de México (RECITES)”

#### 425 **Author contributions**

426 Research idea and study design: RRA, JCGV, OYBC; data acquisition: RRA; data  
427 analysis/interpretation: RRA, JCVG, OYBC; statistical analysis: RRA; manuscript drafting:  
428 RRA, JCGV, OYBC; supervision or mentorship: RRA. Each author contributed important  
429 intellectual content during manuscript drafting or revision and accepted accountability for  
430 the overall work by ensuring that questions about the accuracy or integrity of any portion of  
431 the work are appropriately investigated and resolved.

432

#### 433 **REFERENCES**

- 434 1. Sohrabi C, Alsafi Z, O’Neill N, Khan M, Kerwan A, Al-Jabir A, et al. World Health  
435 Organization declares global emergency: A review of the 2019 novel coronavirus  
436 (COVID-19). *Int J Surg.* 2020 Apr;76:71–76.

- 437 2. Forouzanfar MH, Sepanlou SG, Shahrzad S, Dicker D, Naghavi P, Pourmalek F, et al.  
438 Evaluating causes of death and morbidity in Iran, global burden of diseases, injuries,  
439 and risk factors study 2010. *Arch Iran Med*. 2014 May;17(5):304–320.
- 440 3. Johns Hopkins Coronavirus Resource Center - Johns Hopkins Coronavirus  
441 Resource Center [Internet]. [cited 2020 Apr 17]. Available from:  
442 <https://coronavirus.jhu.edu/map.html>
- 443 4. Eden J-S, Rockett R, Carter I, Rahman H, de Ligt J, Hadfield J, et al. An emergent  
444 clade of SARS-CoV-2 linked to returned travellers from Iran. *Virus Evol*. 2020  
445 Jan;6(1):veaa027.
- 446 5. How Iran Became a New Epicenter of the Coronavirus Outbreak | The New Yorker  
447 [Internet]. [cited 2020 Apr 17]. Available from: [https://www.newyorker.com/news/our-](https://www.newyorker.com/news/our-columnists/how-iran-became-a-new-epicenter-of-the-coronavirus-outbreak)  
448 [columnists/how-iran-became-a-new-epicenter-of-the-coronavirus-outbreak](https://www.newyorker.com/news/our-columnists/how-iran-became-a-new-epicenter-of-the-coronavirus-outbreak)
- 449 6. Lachmann A. Correcting under-reported COVID-19 case numbers. *medRxiv*. 2020  
450 Mar 18;
- 451 7. COVID-19: Iran records 4,585 coronavirus deaths as restrictions eased | Mena –  
452 Gulf News [Internet]. [cited 2020 Apr 17]. Available from:  
453 [https://gulfnews.com/world/mena/covid-19-iran-records-4585-coronavirus-deaths-as-](https://gulfnews.com/world/mena/covid-19-iran-records-4585-coronavirus-deaths-as-restrictions-eased-1.70954074)  
454 [restrictions-eased-1.70954074](https://gulfnews.com/world/mena/covid-19-iran-records-4585-coronavirus-deaths-as-restrictions-eased-1.70954074)
- 455 8. GHO | By country | Iran (Islamic Republic of) - statistics summary (2002 - present)  
456 [Internet]. [cited 2020 Apr 17]. Available from:  
457 <https://apps.who.int/gho/data/node.country.country-IRN>
- 458 9. Bello-Chavolla OY, González-Díaz A, Antonio-Villa NE, Fermín-Martínez CA,  
459 Márquez-Salinas A, Vargas-Vázquez A, et al. Unequal impact of structural health  
460 determinants and comorbidity on COVID-19 severity and lethality in older Mexican  
461 adults: Considerations beyond chronological aging. *J Gerontol A, Biol Sci Med Sci*.  
462 2020 Jun 29;
- 463 10. Armitage R, Nellums LB. Water, climate change, and COVID-19: prioritising those in  
464 water-stressed settings. *Lancet Planet Health*. 2020;4(5):e175.
- 465 11. Gross B, Zheng Z, Liu S, Chen X, Sela A, Li J, et al. Spatio-temporal propagation of  
466 COVID-19 pandemics. *medRxiv*. 2020 Mar 27;
- 467 12. Chipeta MG, Giorgi E, Mategula D, Macharia PM, Ligomba C, Munyenyembe A, et  
468 al. Geostatistical analysis of Malawi's changing malaria transmission from 2010 to  
469 2017. [version 2; peer review: 2 approved, 1 approved with reservations]. *Wellcome*  
470 *Open Res*. 2019 Jul 4;4:57.
- 471 13. Sanna M, Wu J, Zhu Y, Yang Z, Lu J, Hsieh Y-H. Spatial and temporal  
472 characteristics of 2014 dengue outbreak in guangdong, china. *Sci Rep*. 2018 Feb  
473 5;8(1):2344.
- 474 14. Carmo RF, Nunes BEBR, Machado MF, Armstrong AC, Souza CDF. Expansion of  
475 COVID-19 within Brazil: the importance of highways. *J Travel Med*. 2020 Jun 27;

- 476 15. Deutsch-Feldman M, Brazeau NF, Parr JB, Thwai KL, Muwonga J, Kashamuka M, et  
477 al. Spatial and epidemiological drivers of Plasmodium falciparum malaria among  
478 adults in the Democratic Republic of the Congo. *BMJ Glob Health*. 2020 Jun;5(6).
- 479 16. Lin D, Cui Z, Chongsuvivatwong V, Palittapongarnpim P, Chaiprasert A, Ruangchai  
480 W, et al. The geno-spatio analysis of Mycobacterium tuberculosis complex in hot and  
481 cold spots of Guangxi, China. *BMC Infect Dis*. 2020 Jul 1;20(1):462.
- 482 17. Presidency of the I.R.I. Statistical Center of Iran [Internet]. Statistical Center of Iran.  
483 2020 [cited 2020 Jul 22]. Available from: <https://www.amar.org.ir/english/>
- 484 18. Iran Data Portal [Internet]. [cited 2020 Apr 17]. Available from:  
485 <https://irandataportal.syr.edu/>
- 486 19. Performance Evaluation of the Provinces of Iran Reading To the Measures of Freight  
487 and Passenger Transportation [Internet]. [cited 2020 Apr 17]. Available from:  
488 [http://www.ijte.ir/article\\_69681.html](http://www.ijte.ir/article_69681.html)
- 489 20. Islamic Republic News Agency. Iran's coronavirus toll update March 22, 2020  
490 [Internet]. 2020 [cited 2020 Jul 21]. Available from: <http://archive.vn/nVmn5>
- 491 21. First-level Administrative Divisions, Iran, 2015 | Stanford Digital Repository [Internet].  
492 [cited 2020 Sep 17]. Available from: <http://purl.stanford.edu/dv126wm3595>
- 493 22. Rate Transformations and Smoothing Luc Anselin | Semantic Scholar [Internet].  
494 [cited 2020 Apr 17]. Available from: <https://www.semanticscholar.org/paper/Rate-Transformations-and-Smoothing-Luc-Anselin-Lozano-Koschinsky/88d8b02de84f97f556cfe0ef5a91a7df229cf363#paper-header>
- 497 23. Cressie, Noel. *Statistics For Spatial Data* (wiley Classics Library). Revised. Hoboken,  
498 NJ: Wiley-interscience; 1993.
- 499 24. Moran PAP. Notes on continuous stochastic phenomena. *Biometrika*. 1950  
500 Jun;37(1/2):17.
- 501 25. Wrigley N, Cliff AD, Ord JK. *Spatial processes: models and applications*. *Geogr J*.  
502 1982 Nov;148(3):383.
- 503 26. Anselin L. Local Indicators of Spatial Association-LISA. *Geogr Anal*. 2010 Sep  
504 3;27(2):93–115.
- 505 27. Lopes D, Assunção R. Visualizing Marked Spatial and Origin-Destination Point  
506 Patterns With Dynamically Linked Windows. *Journal of Computational and Graphical*  
507 *Statistics*. 2012 Jan;21(1):134–154.
- 508 28. Ward M, Gleditsch K. *Spatial Regression Models*. 2455 Teller Road, Thousand  
509 Oaks California 91320 United States of America : SAGE Publications, Inc.; 2008.
- 510 29. Silvey SD. The lagrangian multiplier test. *Ann Math Statist*. 1959 Jun;30(2):389–407.
- 511 30. Sahafizadeh E, Sartoli S. Estimating the reproduction number of COVID-19 in Iran  
512 using epidemic modeling. *medRxiv*. 2020 Mar 23;

- 513 31. He J, Chen G, Jiang Y, Jin R, He M, Shortridge A, et al. Comparative Analysis of  
514 COVID-19 Transmission Patterns in Three Chinese Regions vs. South Korea, Italy  
515 and Iran. medRxiv. 2020 Apr 14;
- 516 32. Muniz-Rodriguez K, Fung IC-H, Ferdosi SR, Ofori SK, Lee Y, Tariq A, et al.  
517 Transmission potential of COVID-19 in Iran. medRxiv. 2020 Mar 10;
- 518 33. Kraemer MUG, Yang C-H, Gutierrez B, Wu C-H, Klein B, Pigott DM, et al. The effect  
519 of human mobility and control measures on the COVID-19 epidemic in China.  
520 Science. 2020 Mar 25;
- 521 34. Zhou F, Yu T, Du R, Fan G, Liu Y, Liu Z, et al. Clinical course and risk factors for  
522 mortality of adult inpatients with COVID-19 in Wuhan, China: a retrospective cohort  
523 study. Lancet. 2020 Mar 28;395(10229):1054–1062.
- 524 35. Wu JT, Leung K, Bushman M, Kishore N, Niehus R, de Salazar PM, et al. Estimating  
525 clinical severity of COVID-19 from the transmission dynamics in Wuhan, China. Nat  
526 Med. 2020 Apr;26(4):506–510.
- 527 36. Santessmasses D, Castro JP, Zenin AA, Shindyapina AV, Gerashchenko MV, Zhang  
528 B, et al. COVID-19 is an emergent disease of aging. medRxiv. 2020 Apr 15;
- 529 37. Kashnitsky I, Aburto JM. COVID-19 in unequally ageing European regions. 2020 Mar  
530 18;
- 531 38. Liu Q, Cao L, Zhu X-Q. Major emerging and re-emerging zoonoses in China: a  
532 matter of global health and socioeconomic development for 1.3 billion. Int J Infect  
533 Dis. 2014 Aug;25:65–72.
- 534 39. Wu T, Perrings C, Kinzig A, Collins JP, Minter BA, Daszak P. Economic growth,  
535 urbanization, globalization, and the risks of emerging infectious diseases in China: A  
536 review. Ambio. 2017 Feb;46(1):18–29.
- 537 40. Kost GJ. Geospatial Hotspots Need Point-of-Care Strategies to Stop Highly  
538 Infectious Outbreaks: Ebola and Coronavirus. Arch Pathol Lab Med. 2020 Apr 16;
- 539 41. Lin Y-H, Liu C-H, Chiu Y-C. Google searches for the keywords of “wash hands”  
540 predict the speed of national spread of COVID-19 outbreak among 21 countries.  
541 Brain Behav Immun. 2020 Apr 10;
- 542 42. Chung RY-N, Dong D, Li MM. Socioeconomic gradient in health and the covid-19  
543 outbreak. BMJ. 2020 Apr 1;369:m1329.
- 544 43. Wang Z, Tang K. Combating COVID-19: health equity matters. Nat Med. 2020  
545 Apr;26(4):458.
- 546 44. Aboubakr HA, Sharafeldin TA, Goyal SM. Stability of SARS-CoV-2 and other  
547 coronaviruses in the environment and on common touch surfaces and the influence  
548 of climatic conditions: a review. Transbound Emerg Dis. 2020 Jun 30;
- 549 45. Jamil T, Alam IS, Gojobori T, Duarte C. No Evidence for Temperature-Dependence  
550 of the COVID-19 Epidemic. medRxiv. 2020 Mar 31;

- 551 46. Kissler SM, Tedijanto C, Goldstein E, Grad YH, Lipsitch M. Projecting the  
552 transmission dynamics of SARS-CoV-2 through the postpandemic period. *Science*.  
553 2020 Apr 14;
- 554 47. Li R, Pei S, Chen B, Song Y, Zhang T, Yang W, et al. Substantial undocumented  
555 infection facilitates the rapid dissemination of novel coronavirus (SARS-CoV2).  
556 *Science*. 2020 Mar 16;
- 557 48. World Population Prospects - Population Division - United Nations [Internet]. [cited  
558 2020 Jul 23]. Available from:  
559 <https://population.un.org/wpp/Download/Probabilistic/Population/>
- 560

## 561 TABLES

562 **Table 1.** Features extracted for spatial analyses disaggregated by Iranian provinces to predict the spread of COVID-19 cases.

563 Abbreviations: GDP, Gross Domestic Product; TEI, Transportation Efficiency Index

Province	Cases <sup>+</sup>	Urban population (%) <sup>*</sup>	>60 years (%) <sup>*</sup>	Area (km <sup>2</sup> ) <sup>*</sup>	Density <sup>*</sup>	Literacy (%) <sup>*</sup>	Average temperature (°C) <sup>*</sup>	Annual precipitation (mm) <sup>*</sup>	Physicians <sup>**</sup>	GDP <sup>**</sup> (2004)	Hospital beds <sup>**</sup> (2006)	Inflation <sup>*</sup>	TEI <sup>***</sup>	Population <sup>****</sup> (2020)
Alborz	906	92.639	8.914	5122	529.559	92.2	16.7	220.5	2632.5	12.577	15327.5	28	0.524	2952309.6
Ardebil	213	68.169	9.371	17800	71.372	83.1	10.9	296.5	354	1.127	1654	23.4	0.46	1287965.6
Bushehr	46	71.854	6.841	22743	51.154	89.2	26.5	272.5	429	3.227	1345	24.4	0.301	1267760.8
Chahar Mahall and Bakhtiari	58	64.092	8.691	16328	58.045	84.7	11.8	309.7	499	0.727	1234	22.7	0.754	989763
East Azarbaijan	571	71.859	10.732	45651	85.642	84.7	14	286.9	1104	3.927	5964	21	0.56	4057677.6
Esfahan	1538	88.019	10.643	107018	47.850	89.9	17.7	96.3	2109	6.527	8261	24.2	0.696	5314080.4
Fars	386	70.119	9.456	122608	39.567	88.8	18.9	271.5	1661	4.527	7154	22.3	0.591	5054966.8
Gilan	924	63.343	13.250	14042	180.223	87.3	17.3	1388.3	1211	2.327	3716	24	0.472	2570553.6
Golestan	351	53.275	7.796	20367	91.757	86.1	18.8	477.8	998	1.527	1769	25.4	0.372	1942263
Hamadan	155	63.123	10.801	19368	89.748	85	13.1	215.7	688	1.627	3089	22.9	0.429	1722206.8
Hormozgan	124	54.707	6.046	70697	25.127	87.8	27.8	152.2	492	2.227	1686	32.1	1	1935000.6
Ilam	120	68.130	8.508	20133	28.816	84.9	18	842.4	145	0.827	875	27.9	1	598205.2
Kerman	127	58.728	7.811	180726	17.511	81.5	17.2	109.8	955	2.527	3325	25.7	0.47	3345302
Kermanshah	152	75.220	10.023	25009	78.069	85.4	16.5	512.8	755	1.627	2922	22.6	0.536	1958199.6
Khuzestan	359	75.453	7.052	64055	73.539	86.3	27.3	269.7	1599	14.627	7511	22.3	0.95	4853540.2
Kohgiluyeh and Buyer Ahmad	45	55.741	7.139	15504	45.991	84.4	15.7	611.1	232	4.027	573	24.1	1	756590.4
Kordestan	189	70.756	9.304	29137	55.016	84.5	15.4	444.4	605	1.127	2155	18.8	0.818	1690503.8
Lorestan	363	64.460	8.830	28294	62.227	83	17.9	535.6	616	1.327	2153	26.7	0.963	1765773.8
Markazi	782	76.935	10.892	29127	49.077	87	15.1	284.8	514	2.327	1866	23.4	0.689	1441887.8
Mazandaran	1494	57.780	11.414	23842	137.723	88.7	18.6	724.7	1585	3.527	4475	25.9	0.269	3451293.2

North Khorasan	100	56.118	8.500	28434	30.354	83.3	14.8	227.4	288	0.727	730	24.7	0.533	859384
Qazvin	526	74.751	8.925	15567	81.824	88.6	15.7	313.7	429	1.427	1403	25.4	0.544	1331517.8
Qom	1074	95.178	7.696	11526	112.119	88.7	19.6	111.6	319	1.127	1493	24.6	1	1404771.8
Razavi Khorasan	661	73.058	8.478	118851	54.139	89.1	17.2	183.4	3328	5.027	9131	20.5	0.658	6786580.2
Semnan	577	79.803	9.978	97491	7.204	91.5	19.5	107.5	493	0.927	1269	22.7	0.868	759273.6
Sistan and Baluchestan	88	48.491	4.886	181785	15.265	76	19.8	103.7	657	1.127	2117	26.5	1	2967563.6
South Khorasan	100	59.023	9.757	95385	8.061	86.8	17.4	144.3	512	0.527	660	24.5	0.605	853989.2
Tehran	4260	93.854	10.443	13692	969.007	92.9	19.1	209.3	2632.5	12.577	15327.5	28	1	14135033.8
West Azarbaijan	300	65.423	8.562	37411	87.280	82	12.5	277.3	993	2.027	3630	23.3	0.644	3412933.4
Yazd	471	85.316	8.788	129285	8.806	90.9	21.3	38.4	610	1.227	2395	23.1	0.941	1189817
Zanjan	261	67.253	9.783	21773	48.568	84.8	14	283.1	492	1.027	1264	22.4	0.651	1090842.6

564 \* Statistical Centre of Iran

565 \*\* Iran data portal

566 \*\*\* Obtained from reference (12)

567 \*\*\*\* Population projected by using the population census 2011 and 2016 and an arithmetic method

568 †Cases obtained from John Hopkins Database (<https://coronavirus.jhu.edu/map.html>)

569 **Table 2.** Spatial lag models estimated via maximum likelihood to predict log-transformed COVID-19 case distribution between Iranian  
 570 provinces (model including all variables and model obtained through a selection scheme).

Variable	Coefficient		SE		z-value		p-value	
	All variables*	Selection scheme**	All variables	Selection scheme	All variables	Selection scheme	All variables	Selection scheme
<b>Spatial parameter (<math>\rho</math>)</b>	0.723	0.737	0.107	0.104	6.734	7.069	<0.001	<0.001
<b>Model constant</b>	2.510	2.853	2.550	2.425	0.984	1.176	0.325	0.239
<b>Urban population (%)</b>	0.026	0.026	0.011	0.010	2.345	2.653	0.019	0.008
<b>Population aged <math>\geq 60</math></b>	0.383	0.331	0.075	0.062	5.089	5.324	<0.001	<0.001
<b>Population density</b>	-0.0002		0.0007		-0.258		0.797	
<b>Literacy</b>	-0.110	-0.103	0.040	0.040	-2.771	-2.591	0.006	0.010
<b>Average temperature (<math>^{\circ}\text{C}</math>)</b>	0.113	0.114	0.030	0.028	3.748	4.105	<0.001	<0.001
<b>Precipitation levels (mm)</b>	-0.0003		0.0003		-0.98		0.327	
<b>Physician distribution</b>	0.0008	0.0008	0.0001	0.0001	5.740	5.746	<0.001	<0.001
<b>GDP</b>	-0.051	-0.057	0.038	0.034	-1.343	-1.699	0.179	0.089
<b>Consumer Price Index</b>	0.032		0.039		0.812		0.417	
<b>TEI</b>	0.157	0.155	0.074	0.074	2.112	2.081	0.035	0.038

\*Likelihood Ratio Test=15.628,  $p < 0.001$  (no spatial vs spatial model);  $R^2=0.877$ ;  $AIC=57.165$ ;  $\sigma^2 = 0.146$   
 \*\* Likelihood Ratio Test=18.682,  $p < 0.001$  (no spatial vs spatial model);  $R^2=0.872$ ;  $AIC=52.704$ ;  $\sigma^2 = 0.152$

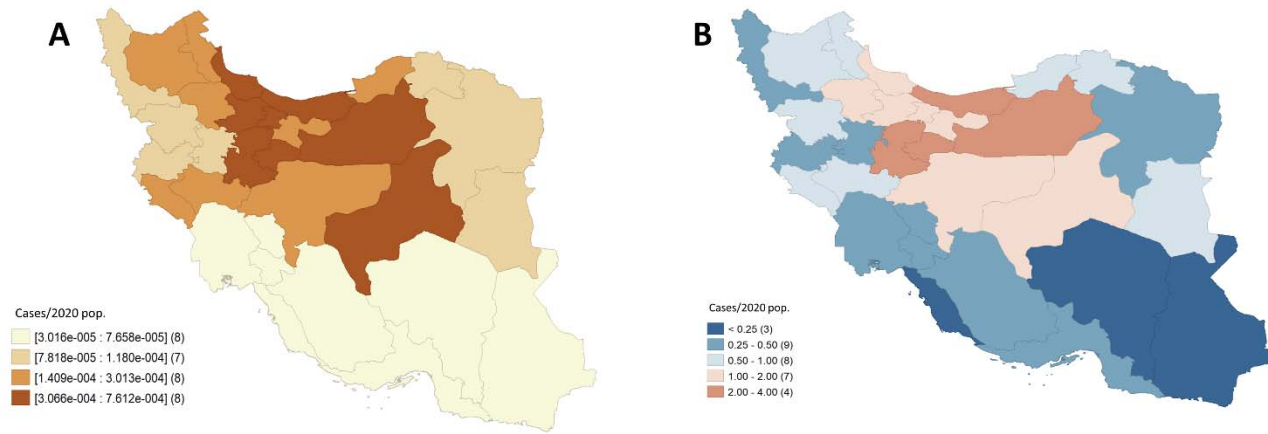
571

572

573



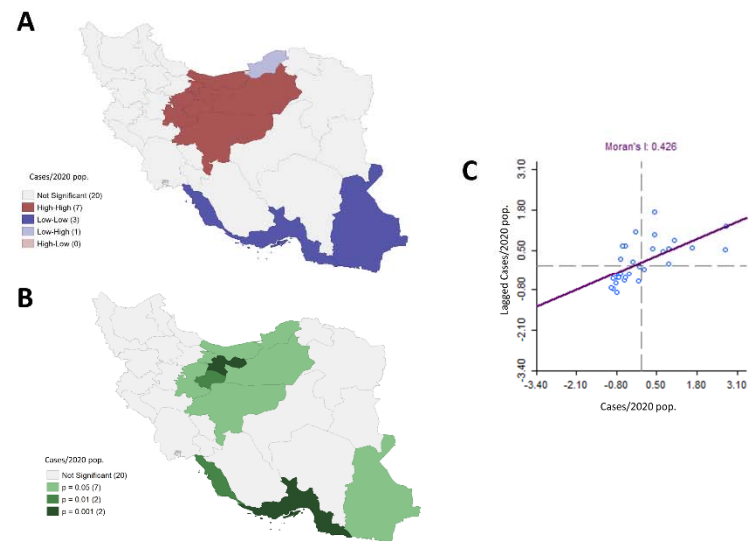
574 **FIGURE LEGENDS**



575

576 **Figure 1. Maps associated with COVID-19 cases by province from February 19th to March 20th, 2020.** A) Quartiles were

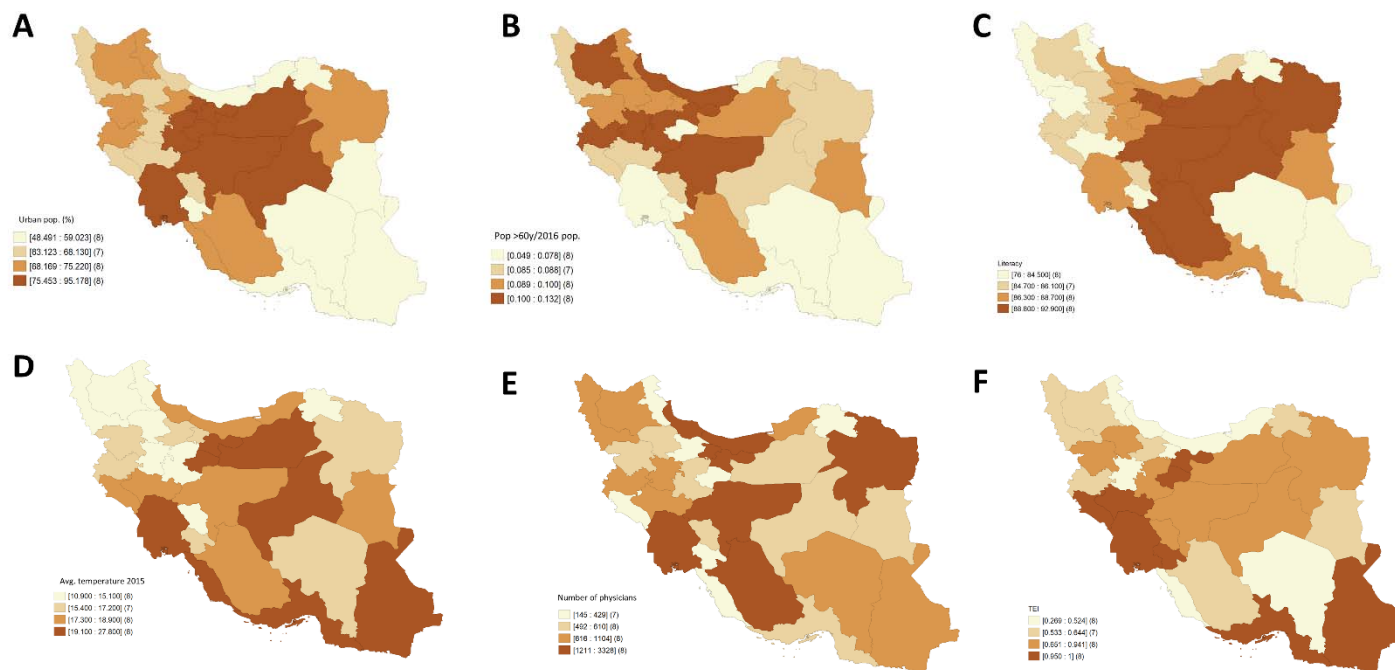
577 corresponding to rates smoothed through an empirical Bayes procedure. B) Excess or relative risk.



578

579 **Figure 2. Spatial clustering associated with rates of COVID-19 cases by province from February 19th to March 20th,**  
580 **considering queen contiguity weights.** A) Significant spatial clustering obtained through Local Indicators of Spatial Autocorrelation  
581 (LISA) comparisons. Four types of a cluster are possible: High-High, Low-Low, High-Low, and Low-High. For instance, the High-High  
582 cluster (red) indicates provinces with high values of a variable that are significantly surrounded by regions with similarly high values.  
583 B) P-values associated with the spatial clustering in A), C) Scatter plot associated with the smoothed rates vs. their corresponding  
584 spatially lagged values, including the associated linear regression fitting, whose slope corresponds to the Moran's I statistic, a global  
585 spatial autocorrelation measure.





587

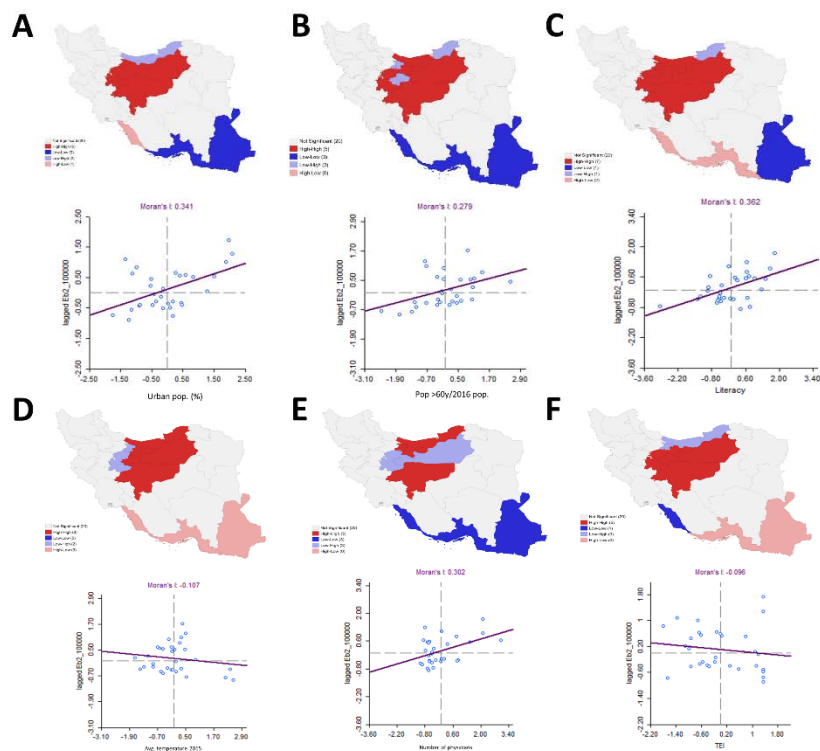
588 **Figure 3. Quartiles associated with all the explanatory variables significant in the spatial lag model with response variable**

589 **the logarithm of the number of COVID-19 cases.** A) People settled in urban areas in 2016 (%). B) People aged  $\geq 60$  years, rates

590 obtained through empirical Bayes smoothing. C) Literacy of population aged  $\geq 6$  years in 2016 (%). D) Average temperature ( $^{\circ}\text{C}$ ) of

591 provincial capitals in 2015. E) Number of physicians employed by the ministry of health and medical education in 2006. F)

592 Transportation Efficiency Index (TEI).



593

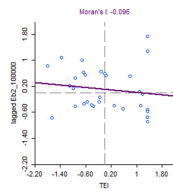
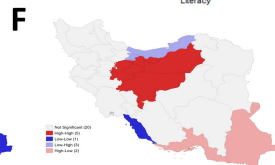
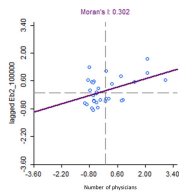
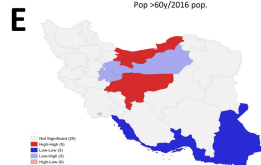
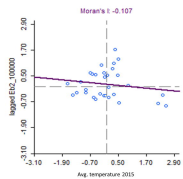
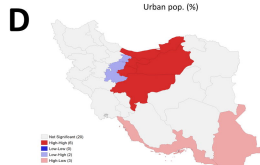
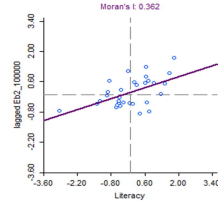
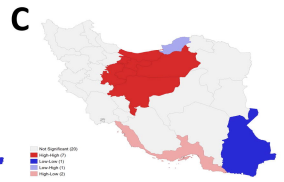
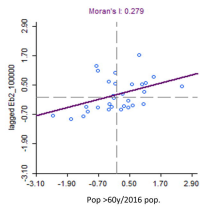
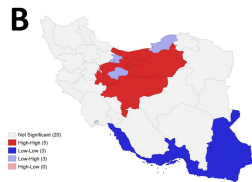
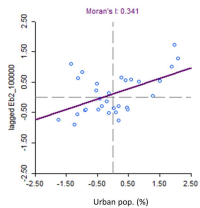
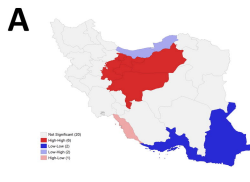
594 **Figure 4. Bivariate LISA's significant spatial clustering between each of the significant variables in the spatial lag model and**  
595 **the rate of cases with COVID-19 smoothed through the empirical Bayes approach.** The scatter plots associated with the  
596 variables vs. the spatially lagged smoothed rate of COVID-19 cases are presented as well, including the associated linear regression  
597 fitting, whose slope corresponds to the bivariate Moran's I statistic, a global spatial bivariate autocorrelation measure. A) People  
598 settled in urban areas in 2016 (%). B) People aged  $\geq 60$  years, rates obtained through empirical Bayes smoothing. C) Literacy of

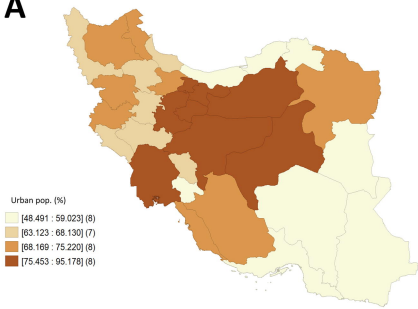
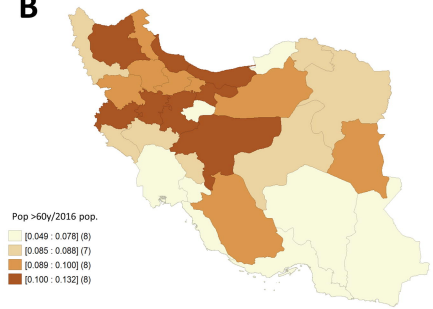
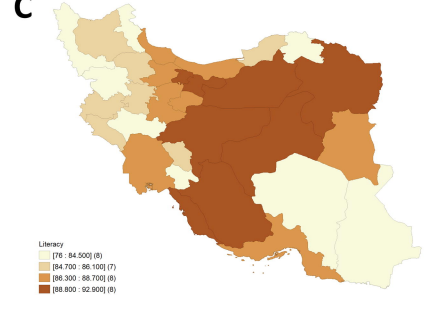
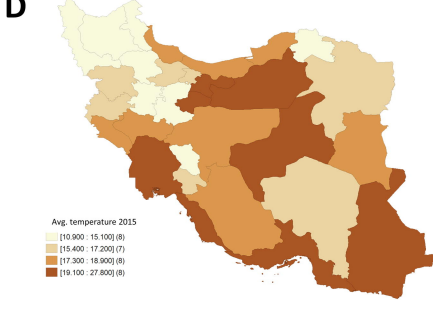
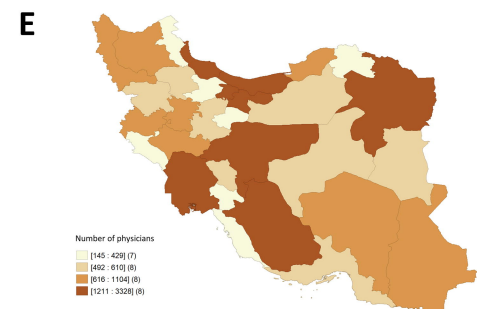
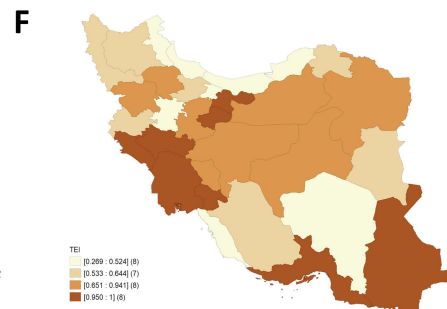
599 population aged  $\geq 6$  years in 2016 (%). D) Average temperature ( $^{\circ}\text{C}$ ) of provincial capitals in 2015. E) Number of physicians employed  
600 by the ministry of health and medical education in 2006. F) Transportation Efficiency Index (TEI).

601

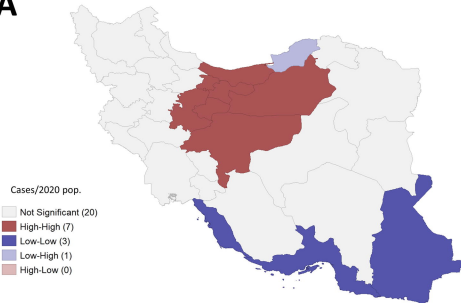
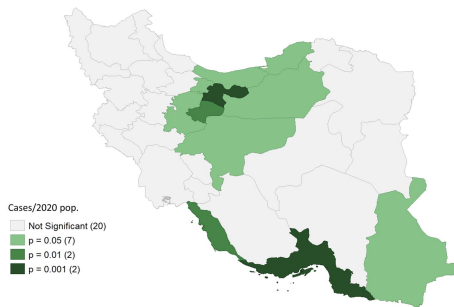
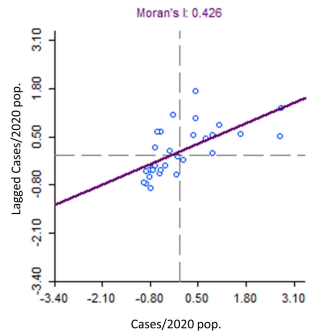
602

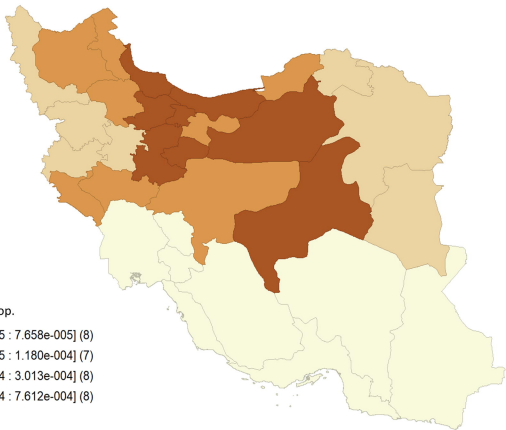
603



**A****B****C****D****E****F**



**A****B****C**

**A****B**